inorganics

MDPI

Article

$RbEr_2AsS_7$: A Rubidium-Containing Erbium Sulfide Thioarsenate(III) with $(S_2)^{2-}$ Ligands According to $RbEr_2S(S_2)[AsS_2(S_2)]$

Katja Engel and Thomas Schleid *

Institute for Inorganic Chemistry, University of Stuttgart, D-70569 Stuttgart, Germany
* Correspondence: thomas.schleid@iac.uni-stuttgart.de; Tel.: +49-711-685-64239

Abstract: The new rubidium-containing erbium sulfide thioarsenate(III) with the structured formula $RbEr_2S(S_2)[AsS_2(S_2)]$ was obtained from the syntheses of elemental erbium (Er), arsenic sesquisulfide (As_2S_3) and rubidium sesquisulfide (Rb_2S_3) with elemental sulfur (S) at 773 K as transparent, orange, needle-shaped crystals. $RbEr_2AsS_7$ crystallizes monoclinically in the space group $C2/c$ with a = 2339.86(12) pm, b = 541.78(3) pm, c = 1686.71(9) pm and β = 93.109(3) ° for Z = 8. The crystal structure features complex $[AsS_2(S_2)]^{3-}$ anions with two S^{2-} anions and a $(S_2)^{2-}$ disulfide dumbbell coordinating end-on as ligands for each As^{3+} cation. Even outside the ligand sphere of As^{3+}, S^{2-} and $(S_2)^{2-}$ can be found as sulfide anions. Two distinct Er^{3+} cations are surrounded by either nine or seven sulfur atoms. The $[ErS_9]$ polyhedra are corner- and face-connected, while the $[ErS_7]$ units share common edges, both building chains along [010]. These different chains undergo edge connectivity with each other, resulting in the formation of corrugated layers, which are held together by Rb^+ in chains of condensed $[RbS_9]$ polyhedra. So, a three-dimensional network is generated, offering empty channels along [010] apt to take up the As^{3+} lone-pair cations. Wavelength-dispersive X-ray spectroscopy verified a molar Rb:Er:As:S ratio of approximately 1:2:1:7 and diffuse reflectance spectroscopy showed the typical f–f transitions of Er^{3+}, while the optical band gap was found to be 2.42 eV.

Keywords: lanthanoids; sulfides; disulfides; thioarsenates; crystal structure

Citation: Engel, K.; Schleid, T. $RbEr_2AsS_7$: A Rubidium-Containing Erbium Sulfide Thioarsenate(III) with $(S_2)^{2-}$ Ligands According to $RbEr_2S(S_2)[AsS_2(S_2)]$. *Inorganics* **2023**, *11*, 465. https://doi.org/10.3390/inorganics11120465

Academic Editor: Hans Riesen

Received: 31 October 2023
Revised: 23 November 2023
Accepted: 27 November 2023
Published: 1 December 2023

1. Introduction

Since lanthanoid-containing thiophosphates show a huge variety of compositions, structures and chemical and physical properties, and arsenic is the next heaviest congener of phosphorus in the periodic system of the elements (PSE), it appears reasonable to assume that similar structures and compositions could be expected for thioarsenates. For a better overview, the system of alkali metal-containing lanthanoid thiophosphates can be subdivided with regard to the oxidation state of phosphorus. In the case of P^{5+}, different compositions of $A_xLn_y[PS_4]_z$ (A = Li, K, Rb Cs; Ln = lanthanoids) are known, e.g., $Li_6Ln_3[PS_4]_5$ with Ln = Y, Gd, Dy and Lu [1]; $K_3Ln[PS_4]_2$ with Ln = La, Ce and Nd [2–4]; $Rb_3Sm[PS_4]_2$ [5]; and $Cs_3Ln_5[PS_4]_6$ with Ln = La and Ce [6]. All these *ortho*-thiophosphates are based on the same thiophosphate(V) anion $[PS_4]^{3-}$, where P^{5+} is tetrahedrally coordinated by four S^{2-} anions. At this point, it should be emphasized that no lanthanoid-containing *ortho*-thiophosphates are known so far with A = Na, which is surprising, since they occur with both direct group neighbors, A = Li and K. Instead, *hypo*-thiodiphosphates $NaLn[P_2S_6]$ with Ln = La–Pr, Sm, Tb, Yb and Lu are formed with phosphorus in the oxidation state +IV, featuring a P–P single bond [7–9]. Thus, since for A = Li, only *ortho*-thiophosphates(V), and for A = Na, only *hypo*-thiodiphosphates(IV) exist, potassium is the first of the alkali metals to form both *ortho*-thio- and *hypo*-thiodiphosphates, followed by A = Rb and Cs, with $KLn[P_2S_6]$ (Ln = La–Pr and Sm), $RbLa[P_2S_6]$ and $CsCe[P_2S_6]$ as examples, in addition to the earlier mentioned *ortho*-thiophosphates [3,7,9,10]. Moreover, even mixed valent compounds, such

as $Rb_4Ln_2[P_2S_6][PS_4]_2$ with *Ln* = La–Nd, Sm and Gd containing both $[P_2S_6]^{4-}$ and $[PS_4]^{3-}$ anions with phosphorus in oxidation states of +IV and +V are known [11]. It can thus be stated that, within the quaternary system of alkali metal-containing lanthanoid(III) thiophosphates, phosphorus occurs preferentially in the +V and +IV oxidation states, but never with +III. For the ternary system of lanthanoid(III) thiophosphates, this statement can even be restricted to the *ortho*-thiophosphates, which contain only P^{5+} cations according to $Ln[PS_4]$ [12–14].

For the analogous systems of alkali metal-containing lanthanoid(III) thioarsenates, the question arises of whether derivatives with As^{5+} are preferentially formed, especially since the ternary lanthanoid(III) *ortho*-thioarsenates(V) $Ln[AsS_4]$ have not been successfully prepared so far, or whether As^{3+} prevails and thus a stronger relationship to thioantimonates(III) occurs. Initial research in the system K/*Ln*/As/S (*Ln* = Nd, Sm, Gd, Dy) showed that tetrahedrally coordinated As^{5+} cations are likely to be preferred [15,16]. Also, for cesium, representatives of the thioarsenates(V) with the composition $Cs_3Ln[AsS_4]_2$ (*Ln* = La–Nd and Sm), the structure of which is dominated by isolated tetrahedral $[AsS_4]^{3-}$ anions, have been prepared successfully in the past [17]. However, lanthanoid(III)-containing thioarsenates can also be synthesized with As^{3+} cations coordinated pyramidally by three S^{2-} anions, e.g., in $Ln_3S_2Cl_2[AsS_3]$ with *Ln* = La and Pr or $CsCeCl_2[AsS_3]$ [18,19], featuring discrete ψ^1-tetrahedral $[AsS_3]^{3-}$ pyramids with a stereochemically active lone pair of electrons at each As^{3+} cation. However, $Cs_4Pr_2[AsS_3]_2[As_2S_5]$ was the first member of the alkali metal-containing lanthanoid(III) thioarsenates(III) to be synthesized without halide participation, containing both isolated $[AsS_3]^{3-}$ anions as well as $[As_2S_5]^{4-}$ units with a sulfide bridge between them [20]. Additionally, trivalent phosphorus in discrete or condensed ψ^1-tetrahedral $[PS_3]^{3-}$ anions is still unknown within the systems under consideration here. So, at first glance, As^{5+} seems to be preferred in the quaternary systems of alkali metal-containing lanthanoid(III) thioarsenates without extra halide anions and *hypo*-thioarsenates(IV) with tetravalent arsenic displaying the $[As_2S_6]^{4-}$ anion with a As–As single bond have been never observed in these systems. In the special case of europium, the exclusive presence of divalent Eu^{2+} cations in $KEu[AsS_3]$ and $KEu[AsS_4]$ have been found, and the crystal structures show on the one hand, pyramidally coordinated As^{3+}, and tetrahedrally coordinated As^{5+} cations on the other [16,21]. Because of these results, the authors postulated a less oxidizing arsenic-rich flux to stabilize As^{3+} in the *A*/Eu/As/S (*A* = Li, K–Cs) systems [21]. Moreover, $Eu_3[AsS_4]_3$ is the only reported ternary compound with divalent europium, but neither $Ln[AsS_4]$ nor $Ln[AsS_3]$ as ternaries with trivalent lanthanoids have been observed yet.

According to the successful attempts of our former research in the systems of alkali metals, lanthanoids, arsenic and sulfur (*A*/*Ln*/As/S, *A* = Rb and Cs) with respect to the formation of $A_3Ln[AsS_4]_2$ compounds with *Ln* = La–Nd and Sm [17], we have now tried to prepare $Rb_3Er[AsS_4]_2$ in analogy to $K_3Gd[AsS_4]_2$ [15]. But the simple change in the synthesis temperature and different sizes of the monovalent counter cations led to single crystals of the new erbium-rich compound $RbEr_2AsS_7$ with the structured formula $RbEr_2S(S_2)[AsS_2(S_2)]$, which includes a rare asymmetric $[AsS_2(S_2)]^{3-}$ anion not documented previously in the lanthanoid-thioarsenates chemistry.

2. Results and Discussion

2.1. Structure Description for $RbEr_2AsS_7$ (≡ $RbEr_2S(S_2)[AsS_2(S_2)]$)

The new rubidium-containing erbium thioarsenate(III) $RbEr_2AsS_7$ crystallizes monoclinically in the space group *C*2/*c* with the lattice parameters *a* = 2339.86(12) pm, *b* = 541.78(3) pm, *c* = 1686.71(9) pm and *β* = 93.109(3)° for *Z* = 8 (Table 1). The structure is composed of only one crystallographically unique rubidium and arsenic cation position each, but two erbium and seven sulfur sites, which are all located at the general *Wyckoff* position 8*f* (Table 2).

Table 1. Crystallographic data for $RbEr_2AsS_7$ and their determination.

Empirical Formula	**$RbEr_2AsS_7$**
Structured formula	$RbEr_2S(S_2)[AsS_2(S_2)]$
Crystal system	monoclinic
Space group	$C2/c$ (no. 15)
Lattice constants	
a/pm	2339.86(12)
b/pm	541.78(3)
c/pm	1686.71(9)
β/°	93.109(3)
Unit cell volume, V_{uc}/nm^3	2.135
Number of formula units	$Z = 8$
Diffractometer	κ-CCD (Bruker-Nonius)
Radiation	Mo-K_α ($\lambda = 71.07$ pm)
Structure solution and refinement	SHELX-97 [22–24]
Index range, $\pm h_{max/} \pm k_{max/} \pm l_{max}$	30/7/21
Number of e$^-$ per unit cell, $F(000)$	2544
Absorption coefficient, μ/mm^{-1}	24.52
Number of collected/unique reflections	28015/2449
$R_{int/}R_\sigma$	0.068/0.028
R_1/wR_2 for all reflections	0.026/0.068
Goodness of fit (GooF)	1.030
Residual electron density, $\rho_{max/min}/10^{-6}$ pm^3	1.64/−1.51
CSD number	2219896

Table 2. Fractional atomic coordinates and coefficients of the equivalent isotropic displacement parameters for $RbEr_2AsS_7$ with all atoms at the symmetry-free *Wyckoff* site 8*f*.

Atom	***x*/*a***	***y*/*b***	***z*/*c***	U_{eq}/pm^2
Rb	0.42638(3)	0.26898(9)	0.41040(4)	299(2)
Er1	0.31925(1)	0.24529(4)	0.08041(2)	150(1)
Er2	0.19026(1)	0.25347(4)	0.22655(2)	149(1)
As	0.06627(3)	0.28248(9)	0.33685(4)	183(2)
S1	0.07440(7)	0.2712(3)	0.20711(9)	213(3)
S2	0.16020(7)	0.2460(3)	0.38410(9)	156(3)
S3	0.43645(7)	0.2077(3)	0.14952(9)	224(3)
S4	0.42774(7)	0.2307(3)	0.02700(9)	227(4)
S5	0.30438(7)	0.2523(3)	0.24007(9)	144(3)
S6	0.20702(7)	0.4488(3)	0.07613(9)	195(4)
S7	0.20447(7)	0.0591(3)	0.07745(9)	201(4)
LP	0.0282	0.2077	0.4047	–

According to the data from the powder X-ray diffraction measurements (PXRD) this compound can also be synthesized from a new mixture of Er:Rb_2S_3:As_2S_3:S with a molar ratio of 4:1:1:8, leading to an almost phase-pure microcrystalline powder, the diffraction data of which match well with those calculated from the single-crystal measurements (Figure 1). The experimental powder diffraction data show several impurities with weak intensities, which could not all be clearly identified. Whereas the excess reflection at $2\theta = 27°$ can be assigned to the main reflection of Rb_2S_3 [25], the second one at $2\theta = 35°$ could not be assigned to a third phase. Washing the crude product with different solvents (e.g., DMSO or DMF) should be tested in the future to avoid possible side phases.

As can be seen from the structured formula $RbEr_2S(S_2)[AsS_2(S_2)]$ (Table 1) and as illustrated in Figure 2, the central structure feature is an isolated complex $[AsS_2(S_2)]^{3-}$ anion, which is built from two S^{2-} anions and one $(S_2)^{2-}$ dumbbell end-on coordinating as a ligand to the central As^{3+} cation. The corresponding As–S distances d(As–S) = 220–232 pm (Table 3) fall into the range of commonly known distances, as, for example, in orpiment As_2S_3 [26]. The angles ∢(S–As–S) = 95–102° within this anion, however, deviate significantly

from those of an ideal tetrahedron (Table 4). This may be due to the stereochemically active lone pair of electrons at the As^{3+} cation on the one hand and the steric influence of the $(S_2)^{2-}$ ligand on the other. This type of complex $[AsS_2(S_2)]^{3-}$ anion has not been reported yet in comparable solids, so, as is known so far, $RbEr_2S(S_2)[AsS_2(S_2)]$ is the first lanthanoid-containing thioarsenate(III) with this structural unit.

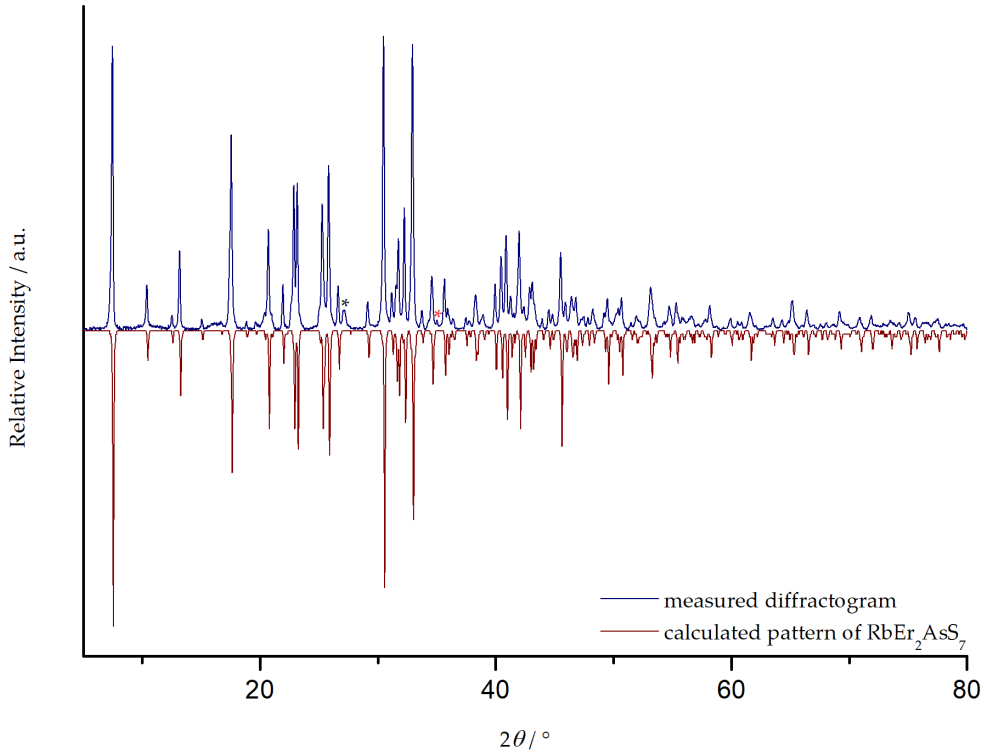

Figure 1. Powder X-ray diffractogram of a microcrystalline powder of $RbEr_2AsS_7$ (blue) and calculated powder pattern of $RbEr_2AsS_7$ from its single-crystal data (red). The black asterisk (*) marks the main reflection of Rb_2S_3, the red one (*) cannot be clearly identified. The unstructured signals around $2\theta = 18°$ result from grease used for sample preparation.

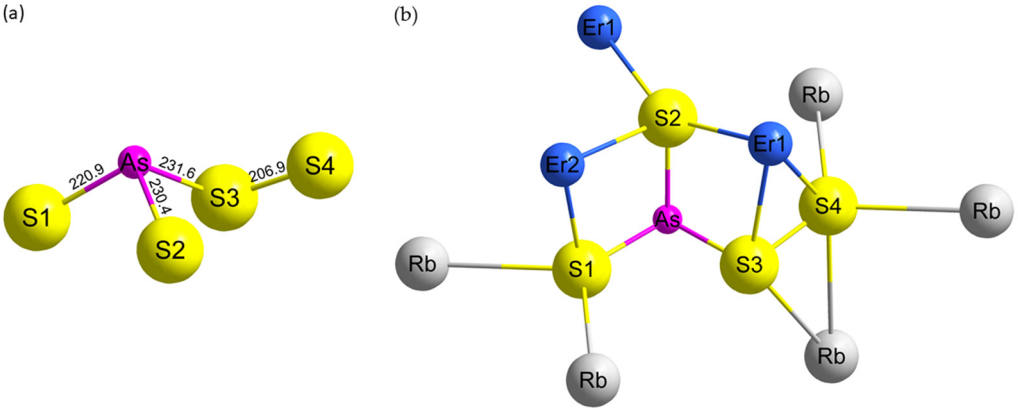

Figure 2. Complex $[AsS_2(S_2)]^{3-}$ anion with given interatomic distances in pm between sulfur (yellow) and arsenic (violet) (**a**) and cationic coordination sphere of the $[AsS_2(S_2)]^{3-}$ anion (**b**) in the crystal structure of $RbEr_2AsS_7$ ($\equiv RbEr_2S(S_2)[AsS_2(S_2)]$), to highlight the connection patterns between the $[AsS_2(S_2)]^{3-}$ anion and the Er^{3+} and Rb^{+} cations in close proximity.

Table 3. Selected interatomic distances in $RbEr_2AsS_7$ ($\equiv RbEr_2S(S_2)[AsS_2(S_2)]$).

Atom Pair	*d*/pm	Atom Pair	*d*/pm
Er1–S5	273.4(1)	Rb–S4	334.5(2)
Er1–S4	274.0(2)	Rb–S1	334.7(2)
Er1–S2	280.6(1)	Rb–S4	334.8(2)
Er1–S2	281.4(1)	Rb–S1	336.6(2)
Er1–S6	284.5(2)	Rb–S3	343.3(2)
Er1–S7	286.7(2)	Rb–S7	345.8(2)
Er1–S6	287.7(2)	Rb–S4	352.4(2)
Er1–S7	289.2(2)	Rb–S6	358.9(2)
Er1–S3	292.8(2)	Rb–S5	394.0(2)
Er2–S5	266.8(2)	As–S1	220.7(2)
Er2–S1	271.5(2)	As–S2	230.5(2)
Er2–S5	276.2(1)	As–S3	231.6(2)
Er2–S7	276.3(2)	*As–LP*	*154*
Er2–S5	277.5(1)		
Er2–S2	278.6(2)	S3–S4	206.9(2)
Er2–S6	279.6(2)	S6–S7	211.2(2)

Table 4. Selected interatomic angles in $RbEr_2AsS_7$ ($\equiv RbEr_2S(S_2)[AsS_2(S_2)]$).

Atom Triple	∢/°
S1–As–S2	102.04(6)
S1–As–S3	97.49(6)
S2–As–S3	94.69(6)
As–S3–S4	99.06(7)

For the charge balance, this complex $[AsS_2(S_2)]^{3-}$ unit is surrounded by five rubidium and three erbium cations (Figure 2b). The end-on coordinating disulfide dumbbell $^{-}$(S3)–(S4)$^{-}$ at the As^{3+} cation is still side-on coordinating the $(Er1)^{3+}$ cation together with two further isolated disulfide dumbbells $^{-}$(S6)–(S7)$^{-}$ and three S^{2-} anions, forming an $[ErS_9]$ polyhedron (Figure 3a, *left*). The two $^{-}$(S6)–(S7)$^{-}$ dumbbells form a rectangular face, via which two $[ErS_9]$ polyhedra are linked. These become additionally corner-connected to their neighboring polyhedra of the same kind and thus form infinite chains $^{1}_{\infty}\left\{(Er1)S^{t}_{3/1}S^{c}_{2/2}S^{f}_{4/2}\right\}$ along [010] (Figure 3a, *right*), with the (Er1)–S distances ranging from 273 to 292 pm (Table 3). The $(Er2)^{3+}$-centered $[(Er2)S_7]$ polyhedra shown in Figure 3b (*left*) are composed by a side-on coordinating disulfide dumbbell $^{-}$(S6)–(S7)$^{-}$ and five S^{2-} anions, including the isolated $(S5)^{2-}$ anion, which is neither part of the coordination environment of As^{3+} nor part of a disulfide dumbbell, and is therefore explicitly emphasized in the structured formula. These distorted pentagonal bipyramids $[ErS_7]$ become linked by their two $(S5)^{2-}$ edges to build up infinite chains $^{1}_{\infty}\left\{(Er2)S^{t}_{4/1}S^{e}_{3/3}\right\}$, which also run along [010] (Figure 3b, *right*). Furthermore, the two erbium-centered polyhedral chains become edge-connected via S2 and S5 and face-connected via S5, S6 and S7 with each other along [001], and thus form corrugated layers $^{2}_{\infty}\left\{[Er_2S_7]^{4-}\right\}$, spreading out parallel to the (100) plane (Figure 4). The (Er2)–S separations of *d*((Er2)–S) = 267–280 pm cover the range of the known distances also found in D-type or F-type Er_2S_3 [27,28], for example. As Figure 2 implies and Figure 5 clearly shows, the isolated $[AsS_2(S_2)]^{3-}$ units are part of these corrugated layers $^{2}_{\infty}\left\{[Er_2S_7]^{4-}\right\}$ via the connection of three Er^{3+}-centered polyhedra, resulting in a two-dimensional anionic layer structure $^{2}_{\infty}\left\{[Er_2AsS_7]^{-}\right\}$ oriented parallel to (100) and separated by Rb^{+} cations.

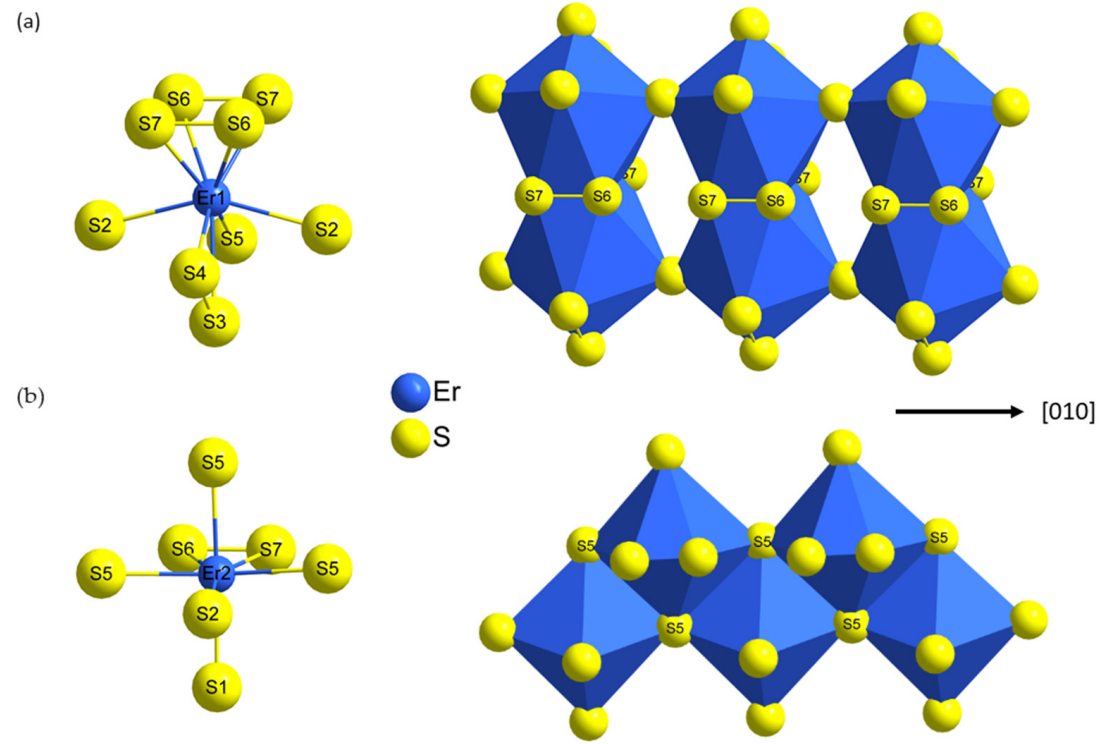

Figure 3. $(Er1)^{3+}$-centered sulfur coordination polyhedron $[(Er1)S_9]$ and condensed polyhedral chains $^1_\infty\left\{(Er1)S^t_{3/1}S^c_{2/2}S^f_{4/2}\right\}$ (**a**) and $(Er2)^{3+}$-centered sulfur coordination polyhedron $[(Er2)S_7]$ and condensed polyhedral chains $^1_\infty\left\{(Er2)S^t_{4/1}S^e_{3/3}S^e_{4/2}\right\}$ (**b**), both propagating along [010].

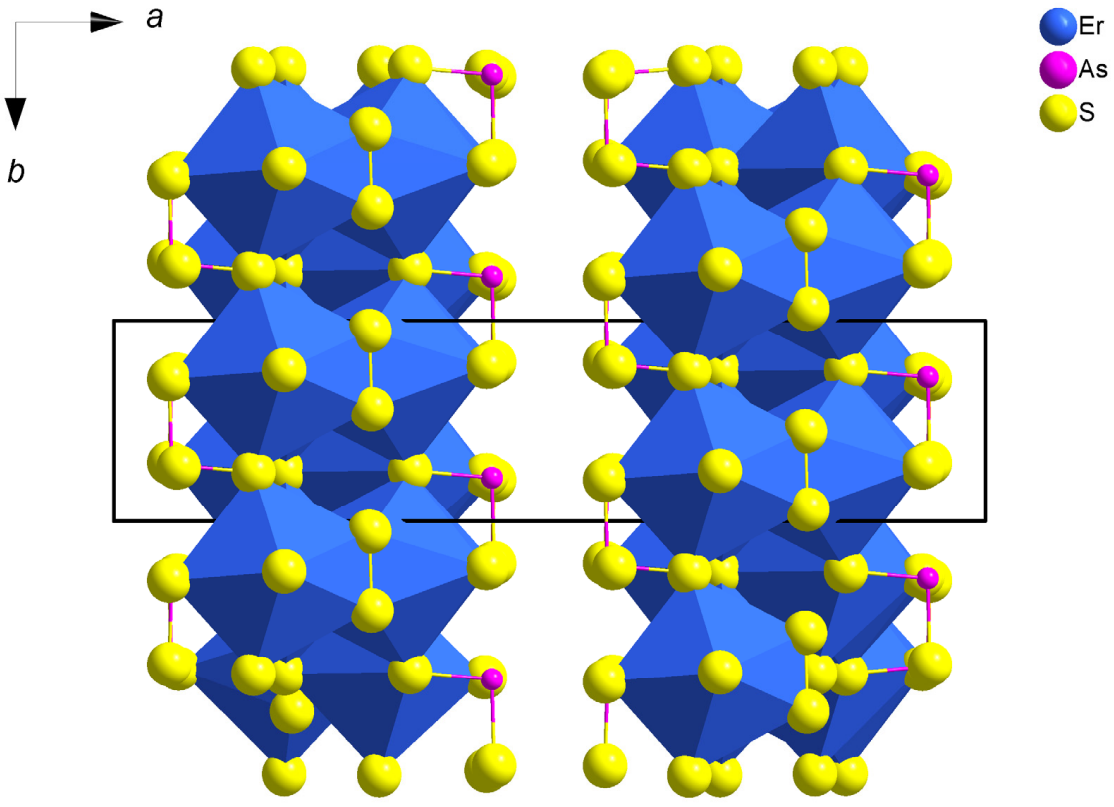

Figure 4. Two-dimensional layer structure built of corrugated $^2_\infty\left\{[Er_2AsS_7]^-\right\}$ slabs spreading out parallel to the (100) plane.

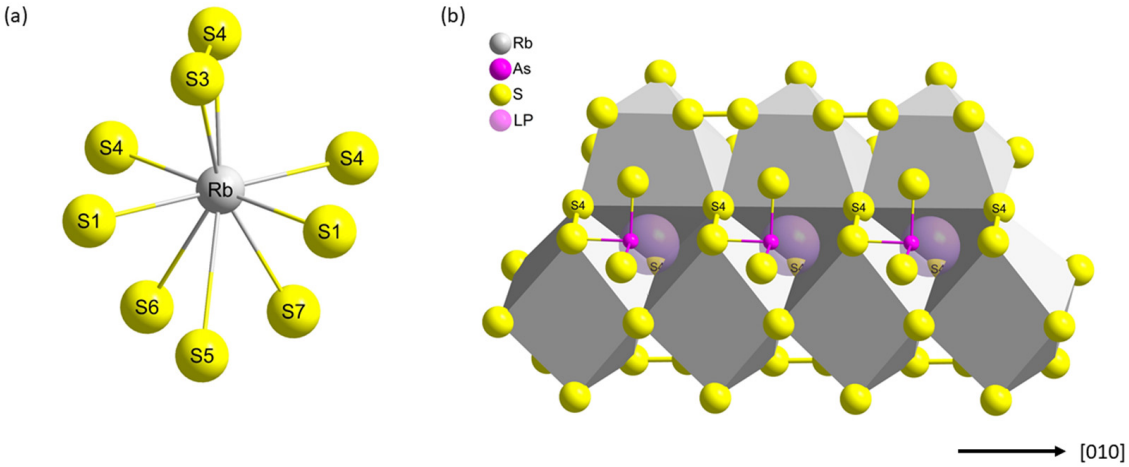

Figure 5. $[RbS_9]$ polyhedron (**a**) and undulated chain of condensed $[RbS_9]$ polyhedra running along [010] with bridging end-on coordinated disulfide dumbbells and As^{3+} cations with their highlighted lone pairs (**b**).

The unique Rb^+ cations are located in the boundary planes of the corrugated Er^{3+}-centered polyhedral sulfur layers, at the centroid of a rectangle spanned by S1···S1···S4···S4. This rectangle is capped by a side-on coordinated disulfide dumbbell $^{-}$(S3)–(S4)$^{-}$ and a triangle spanned by S6···S5···S7, resulting in $[RbS_9]$ polyhedra with d(Rb–S) = 335–394 pm (Figure 5, left). It is worth noting that these polyhedra, on the one hand, form undulated chains by edge connections in $^1_\infty\left\{RbS^t_{4/1}S^e_{2/2}S^e_{3/3}\right\}$ along [010] and are, in addition, bridged by the end-on coordinating disulfide dumbbells $^{-}$(S6)–(S7)$^{-}$ (Figure 5b). As illustrated in Figure 4, the $(S_2)^{2-}$ ligands of the complex thioarsenate(III) anions contribute to the formation of the $[RbS_9]$ polyhedra. In this context, using the numerical calculation program LPLoc [29], the position, radius and distance of the stereochemically active lone pairs (LPs) of the As^{3+} cations were calculated to determine their possible location within the structure. Their radius was calculated to be 115 pm, their atomic coordinates and distances to As^{3+} are given in Tables 2 and 3. The calculation confirms the assumption that the lone pairs are oriented in the direction of the low points in the Rb^+-centered polyhedral chains (Figure 5b). With respect to the earlier mentioned two-dimensional structure built of $^2_\infty\left\{[Er_2AsS_7]^-\right\}$ layers, the overall structure is extended by the Rb^+-centered polyhedra to become a three-dimensional network with empty channels along [010] (Figure 6), if the weak ionic Rb–S bonds are additionally considered.

The crystal structure of the compound is characterized by the rare, non-tetrahedral $[AsS_4]^{3-}$, or, more specifically, the $[AsS_2(S_2)]^{3-}$ anion. This type of complex anion was previously unknown in lanthanoid compounds and could only be realized in solid compounds with tin so far, namely, $KSnAsS_5$ and $Cs_2SnAs_2S_9$ or molecular $[Pt_3(AsS_4)]^{3-}$ and $[Pd_3(AsS_4)_3]^{3-}$ anions [30–32]. Interestingly, in $Cs_2SnAs_2S_9$, this $[AsS_2(S_2)]^{3-}$ anion occurs next to a $[AsS(S_2)_2]^{3-}$ anion that derives from the pyramidal $[AsS_3]^{3-}$ anion through the substitution of two S^{2-} ligands with disulfide dumbbells $(S_2)^{2-}$. From the literature, also for As^{5+}, a complex $[AsS_3(S_2)]^{3-}$ with one disulfide dumbbell as a ligand instead of a spherical S^{2-} anion is known [33]. So, disulfide dumbbells as ligands coordinating to As^{3+} or As^{5+} cations are not something new, but very rare, especially in solids, and were previously unknown in lanthanoid-containing systems. The question arises of why within a system, that previously seemed to favor the formation of tetrahedral $[AsS_4]^{3-}$ anions with pentavalent arsenic, the appearance of the rare $[AsS_2(S_2)]^{3-}$ anion is favored in $RbEr_2S(S_2)[AsS_2(S_2)]$. At this point, the chemistry of arsenic seems to align preferentially with the chemistry of antimony, which prefers the oxidation state +III and for which this type of complex anion is also known, i.e., an analogous $[SbS_2(S_2)]^{3-}$ anion with similar composition is the structural element in $Ba_3Sb_2S_7$ [34,35].

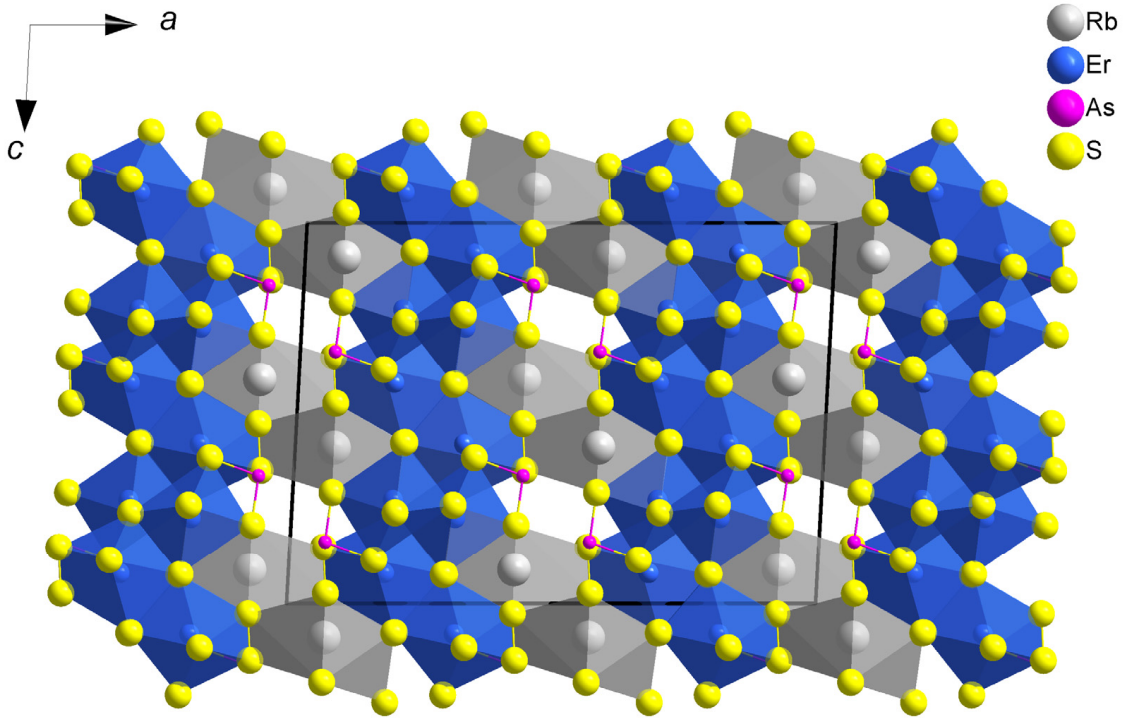

Figure 6. Three-dimensional polyhedral network with empty channels along [010].

2.2. Diffuse Reflectance Spectroscopy (DRS)

Diffuse reflectance UV/Vis measurements were performed to determine the optical band gap of this orange-colored compound. The collected data were transformed using the *Kubelka-Munk* function and plotted in Figure 7 [36]. The optical band gap can be determined by the intersection of the tangents and was found to be 2.42 eV. Furthermore, some bands appear, which are clearly able to be assigned to the *f–f* transitions of Er^{3+} cations by means of the *Dieke* diagram.

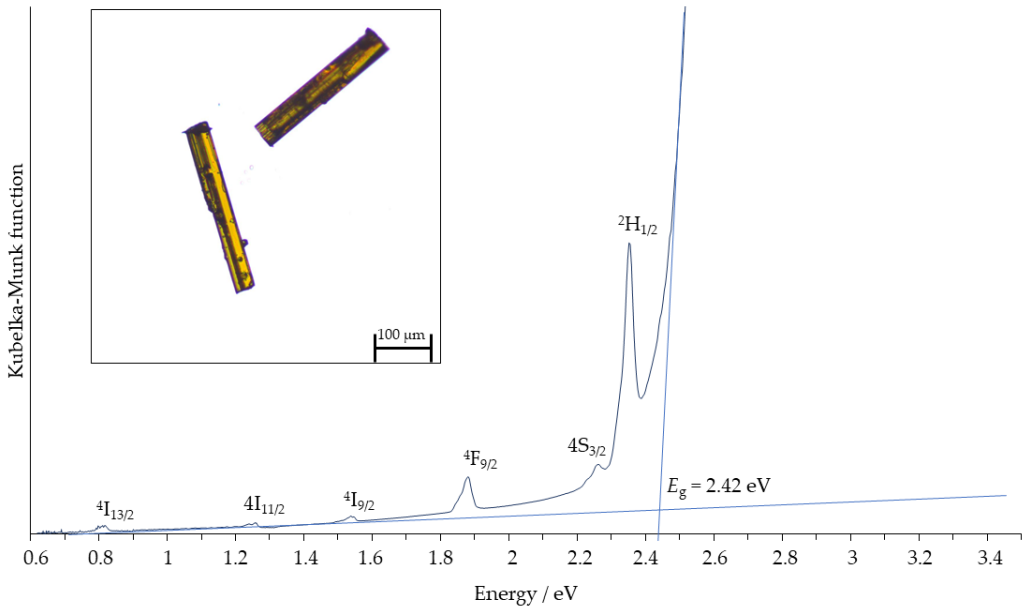

Figure 7. *Kubelka-Munk* plot of the data from diffuse reflectance spectroscopy to determine the optical band gap of $RbEr_2AsS_7$ and orange, needle-shaped crystals of $RbEr_2AsS_7$ (inset).

3. Experimental Section

3.1. Solid-State Synthesis

All preparations and further manipulations were carried out under inert conditions in an argon-filled glove box (GS Mega E-line, Glovebox Systemtechnik, Malsch, Germany). Elemental erbium (Er: 99.9%, ChemPur, Karlsruhe, Germany), arsenic sesquisulfide (As_2S_3: 99.999%, Alfa Aesar, Schwerte, Germany), rubidium sesquisulfide (Rb_2S_3) and elemental sulfur (S: 99+%, ChemPur) were mixed in a molar ratio of 1:1:1:6 expected to yield $Rb_3Er[AsS_4]_2$. The mixture was filled into a fused silica glass ampoule and sealed under dynamic vacuum. The vessel was placed in a computer-controlled muffle furnace (Nabertherm, Lilienthal, Germany) and heated to 773 K within 20 h. After 96 h at 773 K, it was cooled to 523 K at a rate of −2 K/h. This temperature was kept for another 120 h, before cooling down to 373 K at −2 K/h again. At 373 K, the furnace was turned off and allowed to reach room temperature quickly. The trisulfide reagent Rb_2S_3 required for the synthesis was prepared in analogy to Cs_2S_3 from its elements in liquid ammonia [17]. For this purpose, a stoichiometric mixture of elemental rubidium (Rb: 99.5%, ChemPur) and sulfur (S: 99+%, ChemPur) were filled into a pressure-resistant viewing-glass vessel in an argon-filled glove box. This specific container was built with a brass casing with a window, which allows for the observation of the filling level and the reaction's progress. In the brass casing, a thick and stable glass tube (wall thickness: 2 mm) can be placed and closed with a sealing ring made of polytetrafluoroethylene (PTFE) and a connection to a DN 16 small flange. Due to this construction, the vessel is at least resistant against pressure until approximately 12 bar. After filling the solid reactants in that vessel, it was evacuated under exclusion of air at the tensi-eudiometer and subsequently about 6 mL ammonia (99.9999%, Linde Gas GmbH, Pullach, Germany) was condensed into it with the aid of an isopropanol dry ice slush until it was filled to about 50 vol-% with liquid NH_3 [37]. After two days, the conversion of the alkali metal was successfully reached and the synthesis of the yellow-orange colored trisulfide Rb_2S_3 was completed. Due to the moisture sensitivity of this product, it was stored and handled exclusively in a glove box under dry argon.

3.2. Single-Crystal X-ray Diffraction (SCXRD)

The reaction product contained transparent, orange, needle-shaped crystals, which were stable with regard to moist air and water for several weeks. Suitable single crystals were selected for X-ray diffraction measurements (SCXRD) performed on a Bruker-Nonius κ-CCD diffractometer (Karlsruhe, Germany) using monochromatized Mo-K_α radiation (λ = 71.07 pm). For the structure solution and refinement, the program package SHELX-97 was used [22–24]. The monoclinic crystal structure of what turned out to be $RbEr_2AsS_7$ was solved by direct method calculations using the program SHELXS-97 and refined with SHELXL-97 by full matrix least-squares iterations on F^2. Detailed crystallographic data are given in Table 1 and further information of the crystal structure can be obtained from the Cambridge Crystallographic Data Center and the Fachinformationszentrum Karlsruhe service www.ccdc.cam.ac.uk/structures (CSD number: 2219896).

3.3. Wavelength-Dispersive X-ray Spectroscopy (WDXS)

Elemental analysis was performed with an electron-beam X-ray microprobe system (SX-100, Cameca, Gennevilliers, France) equipped with five X-ray wavelength-dispersive spectrometers (WDS). WDXS results for $RbEr_2AsS_7$ confirmed a molar Rb/Er/As/S ratio of approximately 1.0:2.0:1.0:7.1, which agrees well with the single-crystal X-ray structure analysis. For these measurements, single crystals of $RbEr_2AsS_7$ were placed onto a conductive carbon pad (Plano G3347, Wetzlar, Germany) and sputtered with carbon.

3.4. Powder-Crystal X-ray Diffraction (PXRD)

Powder X-ray diffraction patterns were recorded at room temperature on a microcrystalline powder sample (synthesized from a new mixture of Er/Rb_2S_3/As_2S_3/S with the appropriate molar ratio of 4:1:1:8) on a Stoe Stadi-P (Darmstadt, Germany) diffractometer

equipped with a linear PSD Detector and Cu-K_α radiation (λ = 15.42 nm) and matched nicely with the simulated diffractograms from the single-crystal data (Figure 1).

3.5. Diffuse Reflectance Spectroscopy (DRS)

Diffuse reflectance spectroscopy (DRS) on a UV/Vis spectrometer (J&W Tidas, Essingen, Germany) using a finely ground powder without inert gas atmosphere were performed for selecting reflection data and calculating the optical band gap, using the *Kubelka-Munk* function [36].

4. Conclusions

The presented new compound $RbEr_2AsS_7$ with the structured formula $RbEr_2S(S_2)[AsS_2(S_2)]$ represents a hitherto unknown composition in the system of lanthanoid-containing thioarsenates(III) with alkali metal participation. Its crystal structure could be solved from single-crystal X-ray diffraction data, while its composition was confirmed through WDXS measurements. Attempts of phase-pure syntheses using different stoichiometric mixtures of Rb_2S_3, Er As_2S_3 and S led to microcrystalline powder samples, which, according to PXRD, fit well with the data calculated from the SCXRD data. A central building block of the structure is an isolated $[AsS_2(S_2)]^{3-}$ anion, which can be derived from an $[AsS_3]^{3-}$ ψ^1-tetrahedron through the substitution of one S^{2-} ligand with an end-on coordinating $(S_2)^{2-}$ dumbbell. At the same time, the structure contains S^{2-} or $(S_2)^{2-}$ anions that do not belong to the coordination sphere of the As^{3+} cation, but contribute to the formation of the coordination polyhedra about the Er^{3+} and Rb^+ cations, respectively. The Er^{3+} cations are surrounded by either seven or nine sulfur atoms, forming, in total, a two-dimensional structure of corrugated layers $^2_\infty\left\{[Er_2S_7]^{4-}\right\}$ parallel to the (100) plane, apt to accommodate the As^{3+} lone-pair cations according to $^2_\infty\left\{[Er_2AsS_7]^{-}\right\}$. These layers are at least separated by Rb^+ cations, but, with regard to the weak ionic Rb–S bonds, they could also be described as linked by chains of condensed $[RbS_9]$ polyhedra along [010], in which the isolated disulfide dumbbells additionally act as a bridging feature. The resulting three-dimensional network $^3_\infty\left\{[RbEr_2S_7]^{3-}\right\}$ then shows empty channels along [010] for taking up the As^{3+} cations with their lone pairs. Using the LPLoc program to determine the orientation of the stereochemically active lone pairs of the As^{3+} cations, it suggests an alignment of them pointing into the centers of these empty channels.

Since the original target compound would have been $Rb_3Er[AsS_4]_2$ with pentavalent arsenic and tetrahedral $[AsS_4]^{3-}$ anions, as it was successful for the monoclinic series $Rb_3Ln[AsS_4]_2$ (space groups $P2_1/c$ for *Ln* = La and Ce; $P2_1$ for *Ln* = Pr, Nd and Sm; and $C2/c$ for *Ln* = Tb), the question arises of why, in the analogous system of Rb/Er/As/S, the oxidation to As^{5+} did not occur and the prevalence of As^{3+} leaves sulfur behind, ready to oxidize S^{2-} to $(S_2)^{2-}$ ($\equiv {}^-S\text{–}S^-$) inside and outside its coordination sphere. The mentioned results for this $Rb_3Ln[AsS_4]_2$ series will be published in 2024 or later [38].

In conclusion, the new erbium-rich thioarsenate(III) $RbEr_2S(S_2)[AsS_2(S_2)]$ is the first lanthanoid-containing compound with isolated $[AsS_2(S_2)]^{3-}$ polyhedra. This complex thioarsenate(III) anion $[AsS_2(S_2)]^{3-}$ was known in the past in $KSnAsS_5$ and $Cs_2SnAs_2S_9$ or the molecular $[Pd_3(AsS_4)_3]^{3-}$ and $[Pt_3(AsS_4)]^{3-}$ anions, but not in lanthanoid-containing systems [30–32]. Also, the occurrence of S^{2-} and $(S_2)^{2-}$ outside the ligand sphere of As^{3+} represents a new phenomenon in the structural diversity of alkali metal-containing lanthanoid(III) thioarsenates(III).

Author Contributions: Conceptualization, writing of original draft, preparation, SCXRD, PXRD, DRS, WDXS, syntheses, K.E.; supervision, writing and editing, T.S. All authors have read and agreed to the published version of the manuscript.

Funding: We gratefully acknowledge the State of Baden-Württemberg (Stuttgart) for its financial support.

Data Availability Statement: All the data supporting the conclusions are included within the manuscript and available on request from the corresponding authors.

Acknowledgments: We thank Falk Lissner for the single-crystal X-ray diffraction measurement as well as Yanina Dreer and Alexandra Friedly for the WDXS study.

Conflicts of Interest: The authors declare no conflict of interest regarding this article.

References

1. Müller, C.; Jörgens, S.; Mewis, A. Neue Thiophosphate: Die Verbindungen $Li_6Ln_3(PS_4)_5$ (*Ln*: Y, Gd, Dy, Yb, Lu) und $Ag_3Y(PS_4)_2$. *Z. Anorg. Allg. Chem.* **2007**, *633*, 1633. [CrossRef]
2. Gauthier, G.; Jobic, S.; Brec, R.; Rouxel, J. $K_3CeP_2S_8$: A New Cerium Thiophosphate with One-Dimensional Anionic Chains. *Inorg. Chem.* **1998**, *37*, 2332. [CrossRef]
3. Evenson, C.R.; Dorhout, P.K. Thiophosphate Phase Diagrams Developed in Conjunction with the Synthesis of the New Compounds $KLaP_2S_6$, $K_2La(P_2S_6)_{1/2}(PS_4)$, $K_3La(PS_4)_2$, $K_4La_{0.67}(PS_4)_2$, $K_{9-x}La_{1+x/3}(PS_4)_4$ (x = 0.5), $K_4Eu(PS_4)_2$, and $KEuPS_4$. *Inorg. Chem.* **2001**, *40*, 2884–2891. [CrossRef]
4. Wu, Y.; Bensch, W. Syntheses, structures, and spectroscopic properties of $K_9Nd[PS_4]_4$, $K_3Nd[PS_4]_2$, $Cs_3Nd[PS_4]_2$, and $K_3Nd_3[PS_4]_4$. *Inorg. Chem.* **2008**, *47*, 7523–7534. [CrossRef] [PubMed]
5. Milot, S.; Wu, Y.; Näther, C.; Bensch, W.; Klepp, K.O. Two New Quaternary Thiophosphates with Pseudo One-dimensional Structures: Syntheses and Crystal Structures of $Cs_3Sm[PS_4]_2$ and $Rb_3Sm[PS_4]_2$. *Z. Anorg. Allg. Chem.* **2008**, *634*, 1575–1580. [CrossRef]
6. Klepov, V.V.; Pace, K.A.; Breton, L.S.; Kocevski, V.; Besmann, T.M.; zur Loye, H.-C. Nearly Identical but Not Isotypic: Influence of Lanthanide Contraction on $Cs_2NaLn(PS_4)_2$ (*Ln* = La–Nd, Sm, and Gd–Ho). *Inorg. Chem.* **2020**, *59*, 1905–1916. [CrossRef] [PubMed]
7. Schoop, L.M.; Eger, R.; Kremer, R.K.; Kuhn, A.; Nuss, J.; Lotsch, B.V. Structural Stability Diagram of $ALnP_2S_6$ Compounds (*A* = Na, K, Rb, Cs; *Ln* = Lanthanide). *Inorg. Chem.* **2017**, *56*, 1121–1131. [CrossRef] [PubMed]
8. Klepov, V.V.; Breton, L.S.; Pace, K.A.; Kocevski, V.; Besmann, T.M.; zur Loye, H.-C. Size-Driven Stability of Lanthanide Thiophosphates Grown from an Iodide Flux. *Inorg. Chem.* **2019**, *58*, 6565–6573. [CrossRef]
9. Goh, E.-Y.; Kim, E.-J.; Kim, S.-J. Structure Modification on Quaternary Rare Earth Thiophosphates: $NaYbP_2S_6$, $NaSmP_2S_6$, and $KSmP_2S_7$. *J. Solid State Chem.* **2001**, *160*, 195–204. [CrossRef]
10. Manríquez, V.; Galdámez, A.; Cerda-Monje, A.; Peña, O.; Ávila, R.E. Electrical and magnetic properties of quaternary rare earth thiophosphate: $K_4Sm_2[PS_4]_2[P_2S_6]$. *J. Braz. Chem. Soc.* **2009**, *20*, 1499–1503. [CrossRef]
11. Aslani, C.K.; Breton, L.S.; Klepov, V.V.; zur Loye, H.-C. A series of $Rb_4Ln_2(P_2S_6)(PS_4)_2$ (*Ln* = La, Ce, Pr, Nd, Sm, Gd) rare earth thiophosphates with two distinct thiophosphate units $[P^{V}S_4]^{3-}$ and $[P^{IV}{}_2S_6]^{4-}$. *Dalton Trans.* **2021**, *50*, 1683–1689. [CrossRef] [PubMed]
12. Komm, T.; Gudat, D.; Schleid, T. Die Lanthanid(III)-*ortho*-Thiophosphate(V) vomTyp $M[PS_4]$ (*M* = La–Nd, Sm, Gd–Er): Synthese, Kristallstruktur und ^{31}P-NMR-Untersuchungen. *Z. Naturforsch. B* **2006**, *61*, 766–774. [CrossRef]
13. Cleary, D.; Twamley, B. Synthesis and structure of a new layered phase in the lanthanide thiophosphates: $LuPS_4$. *Inorg. Chim. Acta* **2003**, *353*, 183–186. [CrossRef]
14. Scholz, T.; Pielnhofer, F.; Eger, R.; Lotsch, B.V. Lanthanide *ortho*-thiophosphates revisited: Single-crystal X-ray, Raman, and DFT studies of $TmPS_4$ and $YbPS_4$. *Z. Naturforsch. B* **2020**, *75*, 225–231. [CrossRef]
15. Wu, Y.; Näther, C.; Bensch, W. $K_3Ln(AsS_4)_2$ (*Ln* = Nd, Sm, Gd): The First Rare Earth Thioarsenate Compounds with Infinite Straight $1\infty[Ln(AsS_4)_2]^{3-}$ chains. *Inorg. Chem.* **2006**, *45*, 8835–8837. [CrossRef] [PubMed]
16. Wu, Y.; Bensch, W. Syntheses, crystal structures and spectroscopic properties of $KEu[AsS_4]$, $K_3Dy[AsS_4]_2$ and $Rb_4Nd_{0.67}[AsS_4]_2$. *Solid State Sci.* **2009**, *11*, 1542–1548. [CrossRef]
17. Engel, K.; Schleid, T. Die Serie caesiumhaltiger Thioarsenate(V) der Lanthanoide vom Formeltyp $Cs_3Ln[AsS_4]_2$ mit *Ln* = La − Nd und Sm. *Z. Naturforsch. B* **2023**, *in press*.
18. Kang, D.-H. Oxidoarsenate(III/V) und Thioarsenate(III) der Selten-Erd-Metalle. Doctoral Dissertation, Universität Stuttgart, Stuttgart, Germany, 2015.
19. Kang, D.-H.; Schleid, T. $Cs_2CeCl_2[AsS_3]$: Ein neues chlorid-derivatisiertes Caesium-Cer(III)-Thioarsenat(III). *Z. Anorg. Allg. Chem.* **2008**, *634*, 2050. [CrossRef]
20. Ledderboge, F.; Schleid, T. $Cs_4Pr_2As_4S_{11}$: A New Quaternary Thioarsenate(III) According to $Cs_4Pr_2[AsS_3]_2[As_2S_5]$. *Z. Krist. S* **2016**, *36*, 70.
21. Bera, T.K.; Kanatzidis, M.G. $AEuAsS_3$ (*A* = Li, K, Rb, and Cs): New As^{3+} Species from an Arsenic-Rich Polysulfide Flux. *Inorg. Chem.* **2008**, *47*, 7068–7070. [CrossRef]
22. Sheldrick, G.M. *SHELX: Program for Crystal-Structure Solution and Refinement*; University of Göttingen: Göttingen, Germany, 1997.
23. Sheldrick, G.M. A short history of SHELX. *Acta Crystallogr. A* **2008**, *64*, 112–122. [CrossRef] [PubMed]
24. Sheldrick, G.M. Crystal structure refinemement with SHELXL. *Acta Crystallogr. C* **2015**, *71*, 3–8. [CrossRef]
25. Böttcher, P. Darstellung und Kristallstruktur der Dialkalimetalltrichalkogenide Rb_2S_3, Rb_2Se_3, Cs_2S_3 und Cs_2Se_3. *Z. Anorg. Allg. Chem.* **1980**, *461*, 13–21. [CrossRef]

26. Mullen, D.J.E.; Nowacki, W. Refinement of the crystal structures of realgar, AsS, and orpiment, As_2S_3. *Z. Krist.* **1972**, *136*, 48–65. [CrossRef]
27. Schleid, T.; Lissner, F. Einkristalle von A-Nd_2S_3, U-Ho_2S_3, D-Er_2S_3 und E-Lu_2S_3 durch Oxidation reduzierter Chloride der Lanthanide mit Schwefel. *Z. Anorg. Allg. Chem.* **1992**, *615*, 19–26. [CrossRef]
28. Fang, C.M.; Meetsma, A.; Wiegers, G.A.; Boom, G. Synthesis and crystal structure of F-type erbium sesquisulfide, F-Er_2S_3. *J. Alloys Compd.* **1993**, *201*, 255–259. [CrossRef]
29. Hamani, D.; Masson, O.; Thomas, P. Localization and steric effect of the lone electron pair of the tellurium Te^{4+} cation and other cations of the p-block elements. A systematic study. *J. Appl. Cryst.* **2020**, *53*, 1243–1251. [CrossRef]
30. Iyer, R.G.; Kanatzidis, M.G. Controlling Lewis Basicity in Polythioarsenate Fluxes: Stabilization of $KSnAsS_5$ and $K_2SnAs_2S_6$. Extended Chains and Slabs Based on Pyramidal *ß*-$[AsS_4]^{3-}$ and $[AsS_3]^{3-}$ Units. *Inorg. Chem.* **2002**, *41*, 3605–3607. [CrossRef]
31. Iyer, R.G.; Do, J.; Kanatzidis, M.G. Flux Synthesis of the Noncentrosymmetric Cluster Compounds $Cs_2SnAs_2Q_9$ (Q = S, Se) Containing Two Different Polychalcoarsenite *ß*-$[AsQ_4]^{3-}$ and $[AsQ_5]^{3-}$ Ligands. *Inorg. Chem.* **2003**, *42*, 1475–1482. [CrossRef]
32. Chou, J.-H.; Kanatzidis, M.G. Pt^{2+} vs. Pt^{4+} in AsS_3^{3-} Solutions and Isolation of the Clusters $[Pt(As_3S_5)_2]^{2-}$ and $[Pt_3(AsS_4)_3]^{3-}$. Observation of Unique Thioarsenate ligands and Pt–As Bonds. *Inorg. Chem.* **1994**, *33*, 5372–5373. [CrossRef]
33. Iyer, R.G.; Kanatzidis, M.G. $[Mn_2(AsS_4)_4]^{8-}$ and $[Cd_2(AsS_4)_2(AsS_5)_2]^{8-}$: Discrete Clusters with High Negative Charge from Alkali Metal Polythioarsenate Fluxes. *Inorg. Chem.* **2004**, *43*, 3656–3662. [CrossRef]
34. Wang, J.; Lee, K.; Kovnir, K. Synthesis, Crystal, and Electronic Structure of $Ba_3Sb_2Q_7$ (Q = S, Se). *Z. Anorg. Allg. Chem.* **2015**, *641*, 1087–1092. [CrossRef]
35. Zhao, H.-J.; Liu, P.-F. $Ba_3[LiSbS_2(S_2)_2Cl_2]$: The first zero-dimensional (0D) lithium metal thioantimonate featuring molecular anions of $[LiSbS_2(S_2)_2Cl_2]^{6-}$. *J. Solid State Chem.* **2021**, *294*, 121873. [CrossRef]
36. Kubelka, P.; Munk, F. An article on optics of paint layers. *Z. Tech. Phys.* **1931**, *12*, 259–274.
37. Hüttig, G.F. Apparat zur gleichzeitigen Druck- und Raummessung von Gasen (Tensi-Eudiometer). *Z. Anorg. Allg. Chem.* **1920**, *114*, 161–173. [CrossRef]
38. Engel, K. Einblicke in die Welt der Lanthanoid-Thioarsenate: In preparation. Doctoral Dissertation, Universität Stuttgart, Stuttgart, Germany.